© 2017. Published by The Company of Biologists Ltd | Development (2017) 144, 2907-2913 doi:10.1242/dev.145557

RESEARCH REPORT

A novel function for the IκB inhibitor Cactus in promoting Dorsal nuclear localization and activity in the *Drosophila* embryo

Maira Arruda Cardoso[1,2], Marcio Fontenele[1,3], Bomyi Lim[4], Paulo Mascarello Bisch[2], Stanislav Y. Shvartsman[4] and Helena Marcolla Araujo[1,2,*]

ABSTRACT

The evolutionarily conserved Toll signaling pathway controls innate immunity across phyla and embryonic patterning in insects. In the *Drosophila* embryo, Toll is required to establish gene expression domains along the dorsal-ventral axis. Pathway activation induces degradation of the IκB inhibitor Cactus, resulting in a ventral-to-dorsal nuclear gradient of the NFκB effector Dorsal. Here, we investigate how *cactus* modulates Toll signals through its effects on the Dorsal gradient and on Dorsal target genes. Quantitative analysis using a series of loss- and gain-of-function conditions shows that the ventral and lateral aspects of the Dorsal gradient can behave differently with respect to Cactus fluctuations. In lateral and dorsal embryo domains, loss of Cactus allows more Dorsal to translocate to the nucleus. Unexpectedly, *cactus* loss-of-function alleles decrease Dorsal nuclear localization ventrally, where Toll signals are high. Overexpression analysis suggests that this ability of Cactus to enhance Toll stems from the mobilization of a free Cactus pool induced by the Calpain A protease. These results indicate that Cactus acts to bolster Dorsal activation, in addition to its role as a NFκB inhibitor, ensuring a correct response to Toll signals.

KEY WORDS: NFκB, IκB, Toll, Cactus, Dorsal-ventral patterning, *Drosophila*

INTRODUCTION

The evolutionarily conserved Toll receptor pathway is implicated in the control of development, proliferation and immunity. Toll signals are modulated at many levels, a characteristic that facilitates an assortment of possible outcomes (Mitchell et al., 2016). To understand Toll pathway architecture it is necessary to define quantitatively how each pathway element contributes to the final response. Inhibitor of NFκB (IκB) proteins comprise the Toll responsive complex together with NFκB effectors. Therefore, they are central elements of the Toll pathway that require careful analysis of their effects.

Drosophila is a unique system in which to study how IκB proteins tune Toll responses, as disturbances in IκB function can be analyzed concomitantly across a range of Toll activation levels. During embryogenesis, ventral-lateral activation of maternal Toll receptors leads to a ventral-to-dorsal nuclear gradient of the NFκB/c-Rel protein Dorsal (Dl). Inside the nucleus, the differential affinity of Dl-target genes for Dl enables the spatial control of gene expression along the dorsal-ventral (DV) axis (Rushlow and Shvartsman, 2012). High Toll signals lead to ventral mesodermal gene expression, intermediate signals induce lateral neuroectodermal genes, whereas low signals allow dorsal ectodermal gene expression. Toll signals are transduced through mobilization of adaptor proteins, protein kinase activation, and ultimately phosphorylation and proteasomal degradation of the sole *Drosophila* IκB protein Cactus (Cact). Cact degradation then exposes nuclear localization sequences in Dl and nuclear translocation ensues (Stein and Stevens, 2014).

The amount of nuclear Dorsal (nDl) is used as readout for the level of Toll pathway activation. Quantitative analysis of nDl in fixed and live embryos has shown that the Dl gradient is visible from early blastoderm cycle 9, increasing in amplitude with time until mitotic cycle 14 (Kanodia et al., 2009; Liberman et al., 2009; Reeves et al., 2012). Although the shape and dynamics of the Dl gradient have been described under wild-type conditions, how *cactus* (*cact*) disturbances alter these characteristics has not been investigated. Using quantitative analysis we show that, under specific circumstances, loss of *cact* flattens the nDl gradient, implying that *cact* is able to augment Dl nuclear accumulation in addition to its widely established role in inhibiting Toll signals.

RESULTS AND DISCUSSION

Cact augments responses to high Toll signals

In order to identify how Cact tunes NFκB responses, we investigated the effects of reducing *cact* on Dl nuclear localization and expression of Dl target genes using quantitative fluorescent immunolabeling and *in situ* hybridization. It has previously been reported that the nDl gradient expands and the ventral *twist* (*twi*) expression domain widens in embryos generated from mothers carrying *cact* loss-of-function germline clones (Roth et al., 1991). This effect results from depriving the embryo of Cact protein, which releases Dl inhibition in the cytoplasm. Smaller reductions in *cact* lead to milder effects along the DV axis, as revealed by the embryonic cuticle pattern, gastrulation movements and colorimetric *in situ* hybridization (Govind et al., 1993; Isoda and Nusslein-Volhard, 1994; Roth et al., 1991).

To quantify the effect of reducing *cact*, we progressively decreased maternal Cact activity using a series of loss-of-function allelic combinations (Fig. 1 and Figs S1 and S2). One dose of a strong *cact* loss-of-function allele induces 30% embryo lethality, despite only a mild decrease in the number of amnioserosa cells (*cact*[A2]/+ mothers) (Govind et al., 1993) and no detectable alteration in nDl (Fig. 1B,E,F,I,J and Table S1). Further decreasing *cact* function increases nDl in regions of the embryo that receive intermediate or low Toll signals (Fig. 1B-D): in *cact*[A2]/*cact*[011],

[1]Instituto de Ciências Biomédicas, Federal University of Rio de Janeiro, Rio de Janeiro, RJ 21941-902, Brazil. [2]Instituto de Biofísica Carlos Chagas Filho, Federal University of Rio de Janeiro, Rio de Janeiro, RJ 21941-902, Brazil. [3]Institute of Molecular Entomology, Brazil. [4]Lewis-Sigler Institute for Integrative Genomics, Princeton University, Princeton, NJ 08544, USA.

*Author for correspondence (haraujo@histo.ufrj.br)

M.A.C., 0000-0002-8946-4113; M.F., 0000-0001-8828-3671; H.M.A., 0000-0003-0371-9523

Received 7 October 2016; Accepted 5 July 2017

Development (2017) 144, 2907-2913 doi:10.1242/dev.145557

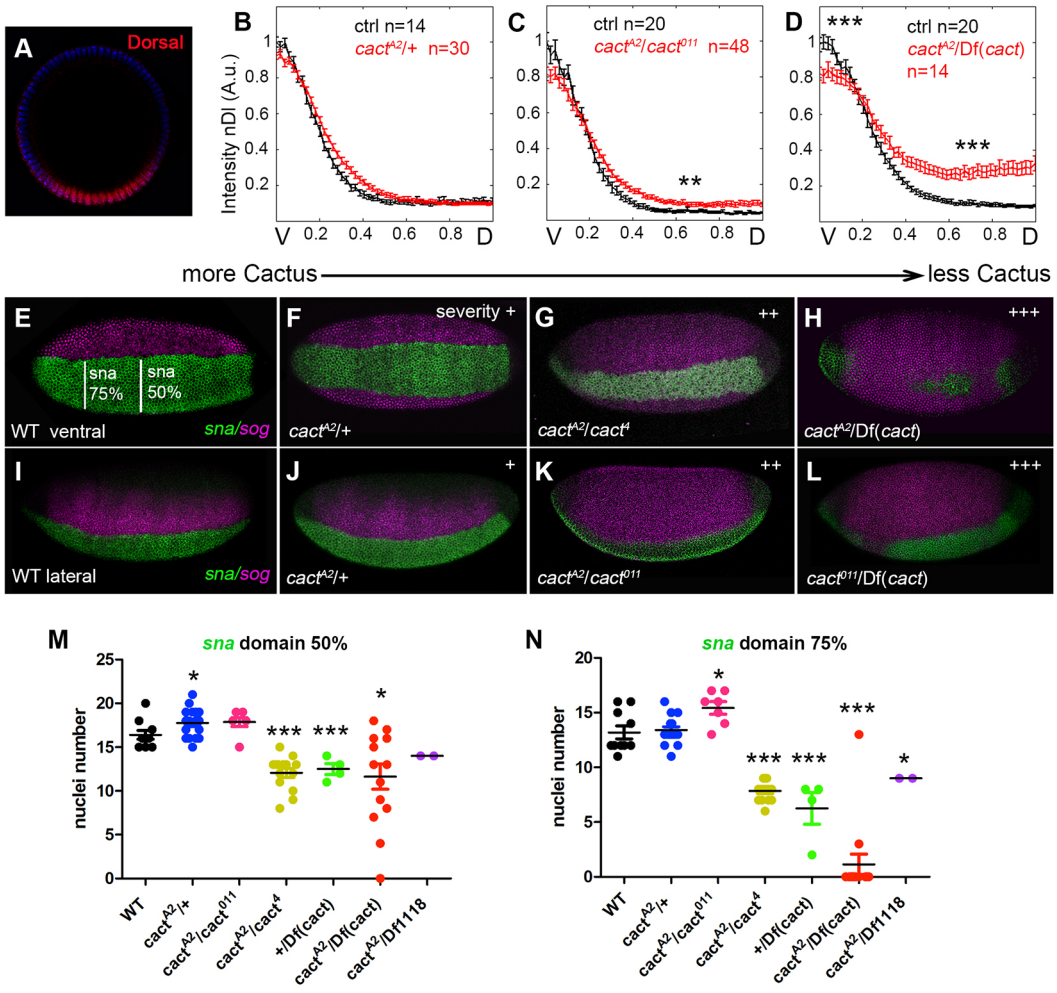

Fig. 1. Cact inhibits Toll in lateral regions and enhances Toll signals in ventral regions of the embryo. (A) Optical section showing a control Dl gradient. (B-D) Nuclear Dl was extracted, measured and plotted as half gradients for control embryos (black) or embryos from *cact*[A2]/+ (B), *cact*[A2]/*cact*[011] (C) or *cact*[A2]/Df(*cact*) (D) mothers (red). The *y* axis represents nDl fluorescence intensity along the ventral-to-dorsal embryonic axis (*x* axis). Data are mean±s.e.m. (E-L) *In situ* hybridization for *sna* (green) in the mesoderm and *sog* (pink) in the lateral neuroectoderm of embryos with maternal *cact* loss-of-function alleles. In embryos from *cact*[011]/+ or *cact* [A2]/+, the ventral and lateral territories are similar to wild type (F,J). Stronger allelic combinations lead to dorsal expansion of lateral *sog* and ventral *sna* reduction in the prospective mesoderm (G,H,K,L). Anterior is leftwards and posterior is rightwards in E-L; dorsal is upwards in G-L. Plus signs in upper right corner indicate the severity of the allelic *cact* combination (+++>++>+), defined by loss of activity and protein levels (Fig. S1). (M,N) The *sna* domain width measured at 50% and 75% egg length. Data are mean±s.e.m. Statistically significant differences were determined using Student's *t*-test (***$P \leq 0.001$, *$P \leq 0.05$).

intermediate (lateral) nDl levels expand to dorsal regions of the embryo (Fig. 1C). These results are in agreement with the embryonic phenotype reported for *cact*[H8] homozygotes (Roth et al., 1991), showing loss of dorsal *zen* gene expression and ventralized cuticles (Table S1 and Fig. S2G). Surprisingly, stronger loss-of-function allelic combinations, as in *cact*[A2]/Df(*cact*) (Fig. 1D), *cact*[A2]/*cact*[4] and *cact*[A2]/Df(2L)III18 (Fig. S2A-C,E) have the same effect on lateral and dorsal territories, but additionally reduce nDl in the ventral domain. As these three genotypes alter *cact* function, their antagonistic effects on ventral and lateral nDl are likely due to *cact*.

The changes in nDl shown above are reflected in the pattern of Dl target genes. The lateral domain of *short gastrulation* (*sog*) expression, a gene that requires intermediate levels of nDl for activation (Stathopoulos and Levine, 2002), expands ventrally and dorsally in several *cact* loss-of-function combinations (Fig. 1G,H,K,L). Dorsal *sog* expansion results from activation by increased nDl, while ventral *sog* expansion probably results from a decrease in nDl and the narrower domain of the Snail repressor. Consistent with this interpretation and with the ventral decrease in nDl, the ventral prospective mesodermal domains of *snail* (*sna*) and *twi* expression, genes that require high levels of nDl for activation (Ip et al., 1991; Papatsenko and Levine, 2005), reduce as Cact activity drops (Fig. 1G,H,L-N, Fig. S2B,C,E and S3B). Therefore, we find that Cact performs an additional function to enhance Toll signals, which is distinct from its established function in inhibiting Dl nuclear translocation.

Next, we investigated whether this positive effect depends on Dl, taking into consideration that the deficiency used in one of the allelic combinations displaying this effect deletes *dl* in addition to *cact* [Df(*cact*)]. In embryos laid by *dl*$^{-}$ heterozygous mothers, nDl decreases ventrally and the *sna* domain narrows compared with wild type (Fig. 2A,C) (Fontenele et al., 2013; Kanodia et al., 2009). We reasoned that decreasing *dl* should sensitize the embryo to Cact reductions if the positive role of Cact depends on Dl. In agreement with this hypothesis, a mild reduction in Cact activity attained in

Development (2017) 144, 2907-2913 doi:10.1242/dev.145557

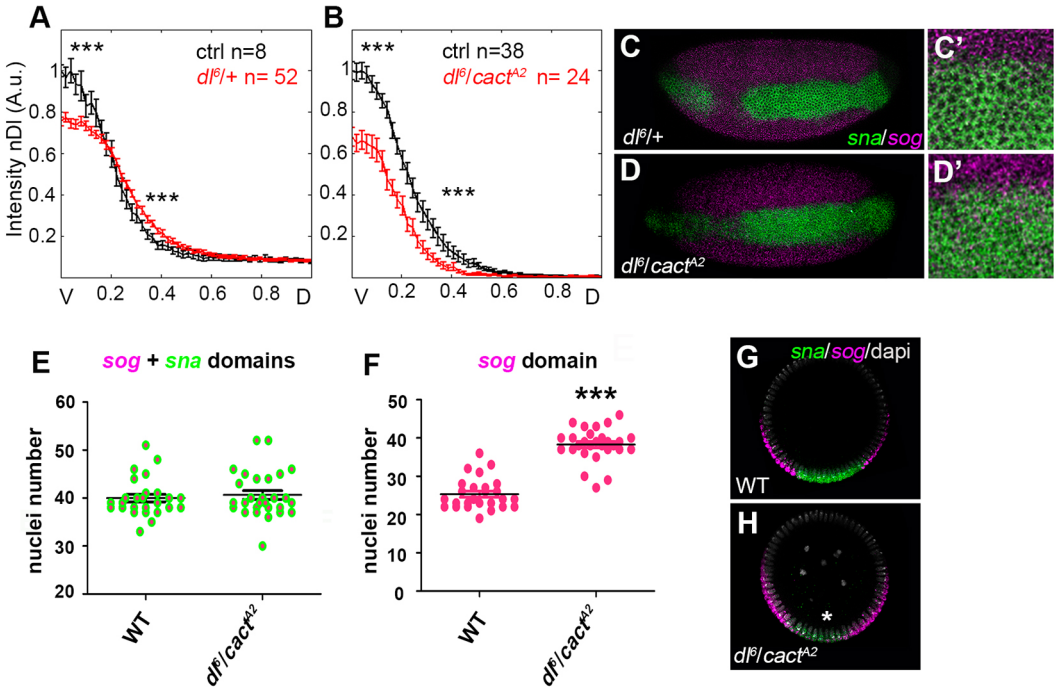

Fig. 2. The ability of Cact to enhance Toll is sensitive to the amount of Dorsal. (A,B) nDl gradients for control embryos (black) or embryos from *dl*[6]/+ (A) or *dl*[6]/*cact*[A2] (B) mothers (red). The nDl gradient decreases by reducing maternal *dl* and *cact*, compared with control embryos stained concomitantly. Data are mean±s.e.m. (C-D′) *In situ* hybridization for *sna* (green) and *sog* (pink) in *dl*[6]/+ (C,C′) or *dl*[6]/*cact*[A2] (D,D′) whole mounts. (C′D′) Higher magnifications of the ventral region showing abbuting ventral *sna* and lateral *sog* domains (C′) versus stochastic *sna* and *sog* in the ventral territory (D′). (E-H) Quantification of *sog*+*sna* domains (E) and *sog* domains alone (F) obtained from wild-type (G) or *dl*[6]/*cact*[A2] (H) transverse sections. Coincident *sog*+*sna* expression is seen in ventral regions in H, unlike wild type or *dl[6]/+*. *sog* domain size measured in E,F includes both left and right sides of the embryo because in *dl*[6]/*cact*[A2] this domain is frequently continuous. Data are mean±s.e.m. Statistically significant differences were determined using Student's *t*-test (***$P \leq 0.001$).

dl[6]/*cact*[A2] significantly decreases nDl in the ventral and lateral domains of the embryo (Fig. 2B). This effect is not observed in *cact*[A2]/+ (Fig. 1B). In addition, in *dl*[6]/*cact*[A2] the lateral *sog* domain expands into the ventral, high Toll activity domain (Fig. 2C-H). Under this condition the ventral *sna* domain is stochastic, enabling ventral *sog* expression in nuclei devoid of the Sna repressor, in agreement with the nDl gradient format (Fig. 2B). However, the total *sog* plus *sna* domain is similar to wild type. In *dl*[6]/*cact*[4] (Fig. S6F), we see a reduction in the *sna* domain compared with *dl*[6]/+, strengthening the hypothesis that the positive role of Cact depends on Dl.

Disturbing the balance between full-length and N-terminal-deleted Cact enhances Toll

Next, as loss of Cact can result in a decrease in nDl, we tested whether altering Cact levels by overexpression results in a corresponding increase in nDl and Dl target genes. Two pathways control Cact levels and activity: Cact is phosphorylated at N-terminal serine residues, ubiquitylated and degraded through the proteasome in response to Toll pathway activation (Bergmann et al., 1996; Fernandez et al., 2001; Hecht and Anderson, 1993; Reach et al., 1996; Shelton and Wasserman, 1993). Cact is also subject to C-terminal CKII kinase phosphorylation through a Toll-independent pathway (Belvin et al., 1995; Liu et al., 1997; Packman et al., 1997), priming Cact for cleavage by the Calpain A (CalpA) protease (Fontenele et al., 2009). N-terminal truncated Cact, hereafter referred to as Cact[E10], is not degraded in response to the Toll pathway. Interestingly, CalpA activity generates Cact[E10], and possibly releases a second full-length free Cact molecule (Fontenele et al., 2013).

To test the effect of increasing Cact activity on the nDl gradient we used gain-of-function alleles and transgenic overexpression lines. The *cact*[E10] and *cact*[BQ] mutants were characterized as gain-of-function alleles that produce N-terminal-deleted proteins that were unresponsive to Toll (Bergmann et al., 1996; Roth, 2001), but that retain their ability to bind Dl (Fontenele et al., 2013). In trans to *cact* loss-of-function alleles, these mutant proteins inhibit Toll pathway activity along the DV axis: the severity of the gain-of-function phenotype increases with severity of the loss-of-function allele (Bergmann et al., 1996; Govind et al., 1993; Roth et al., 1991). In *cact*[E10]/*cact*[A2], the ventral *sna* domain decreases, consistent with Toll pathway inhibition due to *cact*[E10]. Surprisingly, no inhibition is seen dorsally as the lateral *sog* domain remains dorsally expanded, compared with *cact*[A2]/Df(*cact*) (Fig. 3A,B and Fig. 1H). These Dl-target effects are in agreement with nDl gradient alterations (Fig. 3C). Nonetheless, *cact*[E10] and stronger *cact* loss-of-function allelic combinations are lethal, impairing further analysis of a positive effect exerted in the presence of *cact*[E10].

To investigate the effects of altering Cact and Cact[E10] activity, we expressed GFP-tagged Cact chimeric proteins in oocyte and early embryos using a maternal promoter [αtub67C, referred to as CaM (Fernandez et al., 2001)]. In all genetic backgrounds tested, *cact-eGFP* expression either had no effect or decreased nDl levels and the size of Dl-target expression territories, conforming to Cact inhibitory function (Fig. 3D-K and Fig. S4). Importantly, when expressed in a *cact*[A2]/*cact*[011] loss-of-function background, *cact-eGFP* recovers the nDl gradient and reduces lateral *sog* to a wild-type pattern (Fig. S4A,F,I, compare with Fig. 1C), confirming that *CaM>cact-eGFP* produces functional Cact that binds to and inhibits Dl and responds to Toll signals (Fontenele et al., 2013).

Development (2017) 144, 2907-2913 doi:10.1242/dev.145557

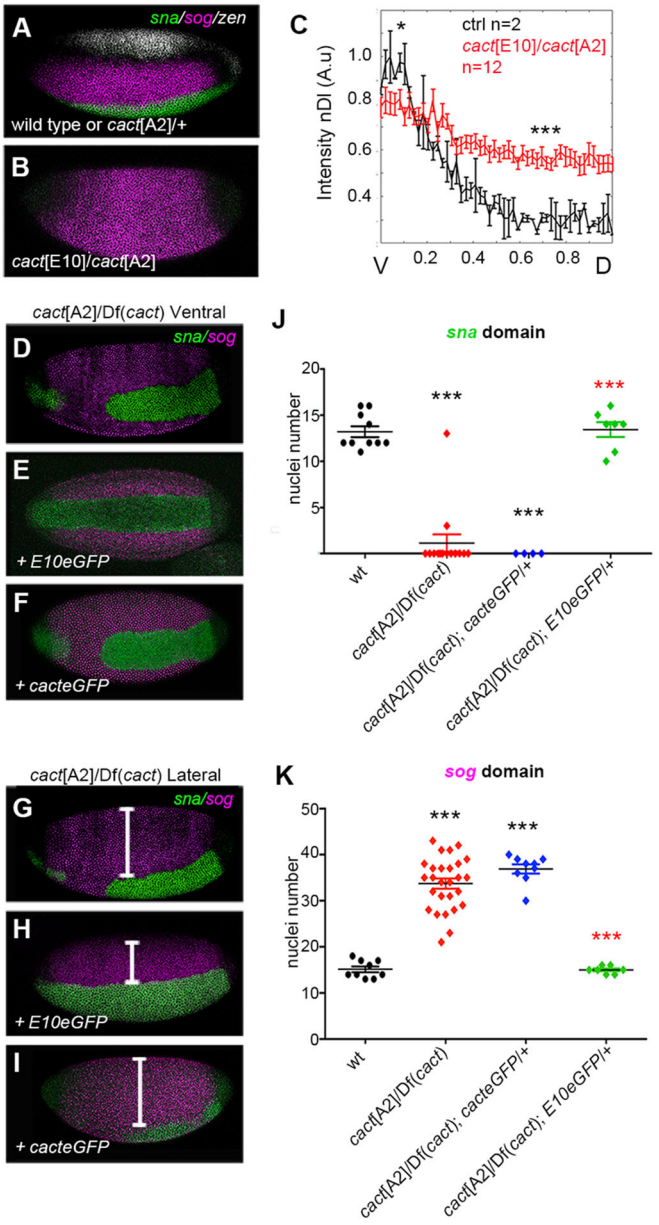

Fig. 3. *cact*[E10] overexpression enhances Toll. (A,B) *In situ* hybridization for *sna*, *sog* and *zen* in wild type (A) and *cact*[E10]/*cact*[A2] (B) showing complete expansion of lateral *sog*. (C) nDl gradients for control embryos (black) or embryos from *cact*[E10]/*cact*[A2] mothers (red). Data are mean±s.e.m. (D-I) *In situ* hybridization for *sna* and *sog* in *cact*[A2]/Df(*cact*) (D,G), *cact*[A2]/Df (*cact*); *cactE10-eGFP*/+ (E,H) and *cact*[A2]/Df(*cact*); *cact-eGFP*/+ (F,I). (J,K) Quantification of *sna* (J) and *sog* (K; bars in G-I) domains at 75% egg length. Full *sog* expansion dorsally is defined when the domain is greater than 25 cells and no dorsal *zen* expression is observed. Data are mean±s.e.m. Statistically significant differences were determined using Student's *t*-test (*$P \leq 0.05$, ***$P \leq 0.001$).

Conversely, *cact[E10]-eGFP* expression increases the ventral *sna* and decreases the lateral *sog* domains that were modified in *cact*[A2]/Df(*cact*) (Fig. 3D,E,G,H,J,K). Therefore, in this genetic background Toll signals enhance ventrally but are inhibited laterally compared with *cact*[A2]/Df(*cact*). This result is consistent with the nDl gradient that reverts to an almost wild-type format (Fig. S5) and akin to the opposing effects shown in *cact* loss-of-function assays (Fig. 1 and Fig. S2 and S3). Importantly, *cact[E10]-eGFP* has no effect on Dl target genes when expressed in the less severe *cact*[A2]/*cact*[011] background (Fig. S4). Thus, the effects of Cact[E10]-eGFP depend on the severity of the *cact* loss-of-function background, similar to the behavior displayed by endogenous *cact* [E10]. This characteristic may stem from differences in functionality of mutant versus wild-type Cact protein, such as different Dl-binding affinities or interactions with other elements of the Toll-dependent and -independent pathways.

The ability of Cact[E10] to alter Toll signals is strongest in the presence of limited Dl, a condition that also reduces endogenous Cact levels (Whalen and Steward 1993; Bergmann et al., 1996). The lateral *sog* domain expands ventrally in *cact*[E10]/*dl*[6] (Fig. S6G-I) due to loss of inhibition by Sna, although no effect is observed in *cact*[E10]/+. Likewise, *cact[E10]-eGFP* has no effect on the nDl gradient in the presence of wild-type Dl levels (Fig. S4C) but produces an inhibitory effect comparable with Cact-eGFP in a dl^{-} heterozygous background (Fig. S6A,B compare with Fig. 2A). Collectively, the results described above indicate the existence of a delicate balance between levels of full-length Cact, truncated Cact (Cact[E10]) and Dl for proper Toll signaling events.

The Toll-independent pathway may implement the positive function of Cact

The phenotypes presented here resulting from *cact* loss-of-function and overexpression alleles show that *cact* is able to enhance Toll signals. Loss of *cact* function results in loss of this positive activity. *cact[E10]eGFP* expression recovers the loss of this positive function, suggesting it acts on the same mechanism that is impaired in specific *cact* allelic combinations. This interpretation is strengthened by the observation that under the loss-of-function and in the *cact*[E10] gain-of-function conditions, the effects are strongest by reducing *cact* and/or *dl*. However, these results raise several questions: by what mechanism does Cact augment Toll signals and what process does *cact*[E10] modify to recover the loss of this positive effect?

First and foremost, endogenous Cact[E10] is a product of the Toll-independent pathway. We have shown that the CalpA protease targets exclusively Dl-free Cact. Our data suggest that CalpA generates Cact[E10] and releases a full-length Cact molecule. Conversely, Cact[E10] inhibits CalpA activity, forming a regulatory loop (Fontenele et al., 2013). Mathematical modeling pointed out the importance of IκB proteins in modulating Toll signals in vertebrates and in *Drosophila sp*. (Ambrosi et al., 2014; Kearns and Hoffmann, 2009; O'Dea et al., 2007). In particular, it was shown that free IκB is an important regulatory target for the control of Toll signals (Konrath et al., 2014). In *Drosophila*, Cact partitions between free and NFκB-bound complexes. Dl-bound Cact corresponds to the Toll-responsive complex (1Cact:2Dl), whereas Dl-free Cact (2Cact) is a target of the Toll-independent pathway (Bergmann et al., 1996; Liu et al., 1997). Taking into account that CalpA enhances Toll signals and produces Cact[E10] from Dl-free Cact, the simplest interpretation of our results is that the positive function attributed to Cact stems from the Toll-independent pathway. Conforming to this hypothesis, CalpA activity is extremely sensitive to Dl and Cact levels, as it is reduced in dl^{-} and $cact^{-}$ (Fontenele et al., 2009, 2013), reminiscent of the positive Cact effects here described.

Notably, vertebrate calpains target IκB proteins, and the pathways that control free and NFκB-bound Cact and IκBα are well conserved (Han et al., 1999; Li et al., 2010; Pando and Verma, 2000; Schaecher et al., 2004; Shen et al., 2001; Shumway et al., 1999). Therefore, our findings of a positive function for Cact may have important implications for the control of vertebrate Toll signals.

Development (2017) 144, 2907-2913 doi:10.1242/dev.145557

Based on the arguments above, we propose a model in which free Cact (unbound to Dl) is modified by the action of CalpA to enhance Toll signals in the embryo by replenishing Cact:2Dl complexes (Fig. 4). However, other mechanisms involving Cact and Cact[E10] could potentially enhance Toll. Appropriate Toll responses depend on pre-signaling complex mobilization (Marek and Kagan, 2012; Sun et al., 2004), endocytosis (Huang et al., 2010; Lund et al., 2010) and DNA-bound NFκB nuclear resident time (Mitchell et al., 2016; O'Connell and Reeves, 2015). Thus, mechanisms involving Cact and Cact[E10] that modify these functions may positively impact Toll signals and explain our results (Fig. 4B). Furthermore, it was recently proposed that Cact functions by a shuttling mechanism to concentrate Dl ventrally (Carrell et al., 2016 preprint), akin to the shuttling mechanism exerted by the BMP inhibitor Sog to concentrate BMPs dorsally (Mizutani et al., 2005; Shimmi et al., 2005; Umulis et al., 2006). Although further research is required to understand how Cact enhances nDl levels in the embryo and consequently Dl-target gene expression, we have clearly shown that Cact exerts a positive effect on Dl nuclear uptake, that this effect is strongest when Dl levels are limiting, and that Cact[E10] modifies an essential process responsible for generating this positive effect. Therefore, we have uncovered a novel function for the Cact inhibitor to enhance Toll responses in the *Drosophila* embryo.

MATERIALS AND METHODS

Fly stocks and genetic crosses

Lines used in this study were: loss-of-function *cact*[A2] and *cact*[011], generously provided by Steve Wasserman; and *dl*[6] and *cact*[4], obtained from the Bloomington Indiana Stock Center. Df(2L)*cact*[255] and Df(2L)III18 were used as *cact* deficiencies. Df(2L)*cact*[255] deletes both *dl* and *cact*, whereas Df(2L)III18 does not delete *dl*. As Df(2L)III18 is not viable in several allelic combinations Df(2L)*cact*[255] was used in most panels unless stated otherwise and is referred to as Df(*cact*). Maternal overexpression lines were CaM>*cact-eGFP* and CaM>*cact*[E10]-*eGFP*, which have been described previously (Fontenele et al., 2013). All embryos were collected from mothers of the respective genotypes crossed with wild-type Canton S males.

Immunoblotting

Bleach dechorionated 30 min- to 1 h 30 min-old embryos of the appropriate genotypes were homogenized in lysis buffer (1 embryo/µl) and prepared for SDS-PAGE as described previously (Fontenele et al., 2009). Endogenous Cact was detected with monoclonal antiserum from Developmental Studies

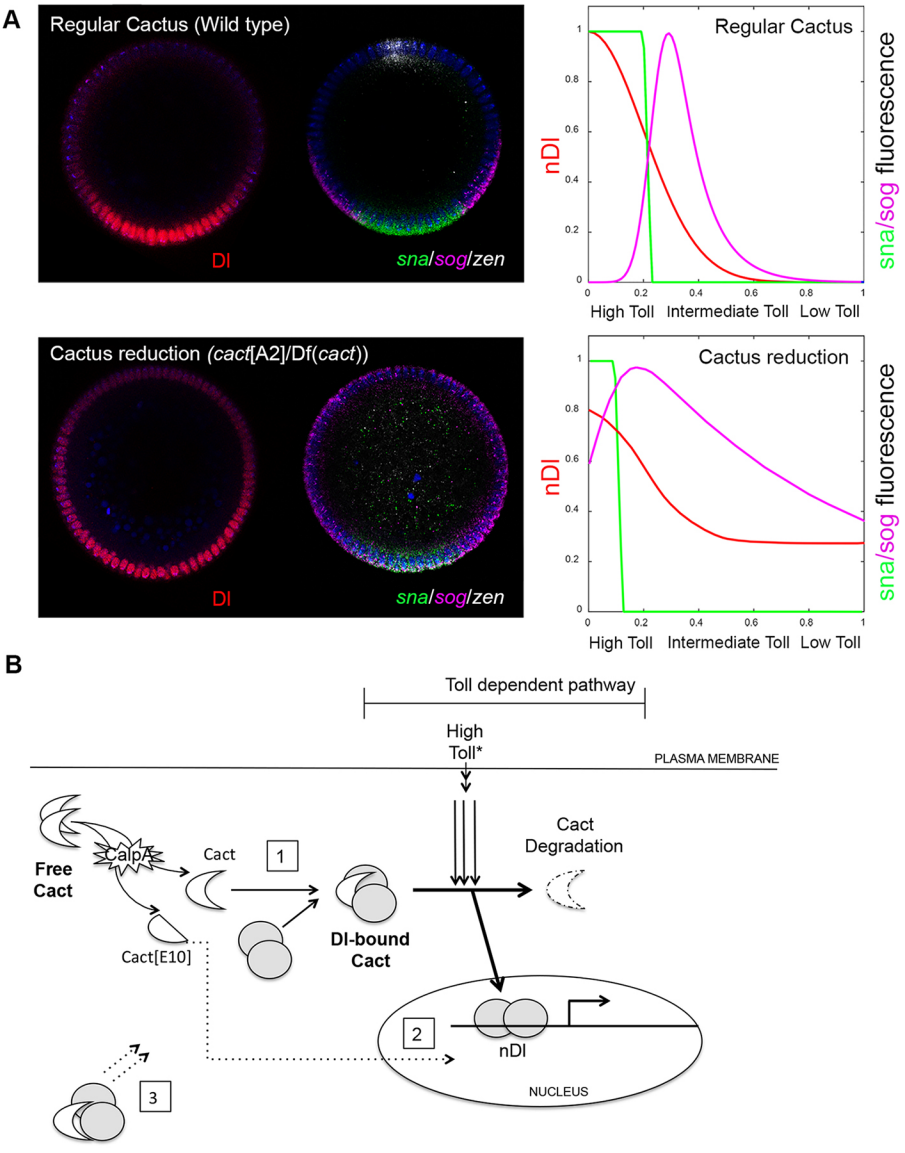

Fig. 4. Model for positive Cact function. (A) nDl (red) and Dl targets (ventral *sna*, green; lateral *sog*, pink; dorsal *zen*, white) in embryo optical cross-sections and graphical representation. Decreasing *cact* function (Cact reduction) results in ventral domain reduction (loss of positive function) and expansion of the lateral territory (loss of inhibitory function). (B) Three possible mechanisms for positive Cact function, based on deploying a Toll-independent pathway: (1) CalpA activity releases Cact[E10] and free full-length Cact, replenishing Dl:Cact signaling complexes that respond to Toll; (2) nuclear Cact[E10], generated by CalpA, increases Dl resident time at promoters; and (3) a flux of free Cact[E10] or free full-length Cact increases Dl diffusion from dorsal to ventral regions of the embryo over time.

Development (2017) 144, 2907-2913 doi:10.1242/dev.145557

Hybridoma Bank (DSHB, anti-Cact, 1:500). Anti-α-Tubulin was used as loading control (DM1α, 1:3000, Sigma). Western blot quantitative data were generated by measuring band intensity relative to tubulin, from direct luminescence using a ImageQuant LAS 4000 (GE Healthcare).

Immunohistochemistry and fluorescent *in situ* hybridization

For nDl gradient visualization, mutant and control Histone-GFP embryos were mixed, fixed and processed concomitantly as described previously (Fontenele et al., 2013). Primary antisera used were monoclonal anti-Dl (7A4, 1:100, DSHB) and anti-GFP (NB600308, 1:1000, Novus Biologicals, to detect control gradients). Dl target genes were visualized by *in situ* hybridization as described previously (Fontenele et al., 2009).

Quantitative analysis

Images of the nDl gradient and Dl target genes were collected from mid-stage 14 embryos, as defined by the amount of membrane invagination around nuclei. Dl gradient quantification was as described previously (Kanodia et al., 2009) using Matlab, collected at 85% egg length using a microfluidic device to orient embryos for end-on imaging (Chung et al., 2011). For upright imaging, a Nikon 60× Plan-Apo oil objective was used, and images were collected at the focal plane ∼90 µm from the embryo anterior pole. For the overall effect on Dl target genes, embryos were imaged laterally. All genotypes were processed and analyzed in parallel; thus, the same wild-type control is shown in graphs. Images were acquired with a Nikon A1 or a Leica LSM confocal microscope.

Statistical analysis

Student's *t*-test was performed for all experiments. Results are displayed as mean±s.e.m. The level of significance is shown in each figure (***$P \leq 0.001$, **$P \leq 0.01$, *$P \leq 0.05$).

Acknowledgements

We thank Trudi Schupbach and Attilio Pane for critical reading of the manuscript, and are greatly indebted to Siegfried Roth for making available essential information on *cact* mutant data. We are grateful to the anonymous reviewers for helpful suggestions to improve the manuscript. Monoclonal antibodies anti-Dl and anti-Cact, originally developed by Ruth Steward, were obtained from the Developmental Studies Hybridoma Bank, created by the NICHD of the NIH and maintained at The University of Iowa, Department of Biology, Iowa City, IA 52242, USA. Stocks obtained from the Bloomington *Drosophila* Stock Center (supported by NIH P40OD018537) were used in this study.

Competing interests

The authors declare no competing or financial interests.

Author contributions

Conceptualization: P.M.B., S.Y.S., H.M.A.; Validation: M.A.C., M.F., B.L.; Formal analysis: M.A.C., M.F., B.L.; Investigation: M.A.C., M.F.; Resources: P.M.B., S.Y.S.; Writing - original draft: M.A.C., H.M.A.; Writing - review & editing: M.A.C., P.M.B., S.Y.S., H.M.A.; Visualization: M.F., H.M.A.; Supervision: P.M.B., S.Y.S., H.M.A.; Project administration: H.M.A.; Funding acquisition: H.M.A.

Funding

This research was funded by the Conselho Nacional de Desenvolvimento Científico e Tecnológico (CNPq-Brazil, 477157/2013-0 to H.M.A.). S.Y.S. was supported by the National Institutes of Health (NIH) (R0 GM107103). M.A.C. was a recipient of Coordenação de Aperfeiçoamento de Pessoal de Nível Superior (CAPES/Brazil) local and overseas fellowships. Deposited in PMC for release after 12 months.

Supplementary information

Supplementary information available online at
http://dev.biologists.org/lookup/doi/10.1242/dev.145557.supplemental

References

Ambrosi, P., Chahda, J. S., Koslen, H. R., Chiel, H. J. and Mizutani, C. M. (2014). Modeling of the dorsal gradient across species reveals interaction between embryo morphology and Toll signaling pathway during evolution. *PLoS Comput. Biol.* **10**, e1003807.

Belvin, M. P., Jin, Y. and Anderson, K. V. (1995). Cactus protein degradation mediates Drosophila dorsal-ventral signaling. *Genes Dev.* **9**, 783-793.

Bergmann, A., Stein, D., Geisler, R., Hagenmaier, S., Schmid, B., Fernandez, N., Schnell, B. and Nüsslein-Volhard, C. (1996). A gradient of cytoplasmic Cactus degradation establishes the nuclear localization gradient of the dorsal morphogen in Drosophila. *Mech. Dev.* **60**, 109-123.

Carrell, S. N., O'Connell, M. D., Allen, A. E., Smith, S. M. and Reeves, G. T. (2016). A facilitated diffusion mechanism establishes the Drosophila dorsal gradient. *bioRxiv* http://dx.doi.org/10.1101/057091.

Chung, K., Kim, Y., Kanodia, J. S., Gong, E., Shvartsman, S. Y. and Lu, H. (2011). A microfluidic array for large-scale ordering and orientation of embryos. *Nat. Methods* **8**, 171-176.

Fernandez, N. Q., Grosshans, J., Goltz, J. S. and Stein, D. (2001). Separable and redundant regulatory determinants in Cactus mediate its dorsal group dependent degradation. *Development* **128**, 2963-2974.

Fontenele, M., Carneiro, K., Agrellos, R., Oliveira, D., Oliveira-Silva, A., Vieira, V., Negreiros, E., Machado, E. and Araujo, H. (2009). The Ca2+-dependent protease Calpain A regulates Cactus/I kappaB levels during Drosophila development in response to maternal Dpp signals. *Mech. Dev.* **126**, 737-751.

Fontenele, M., Lim, B., Oliveira, D., Buffolo, M., Perlman, D. H., Schupbach, T. and Araujo, H. (2013). Calpain A modulates Toll responses by limited Cactus/IkappaB proteolysis. *Mol. Biol. Cell* **24**, 2966-2980.

Govind, S., Brennan, L. and Steward, R. (1993). Homeostatic balance between dorsal and cactus proteins in the Drosophila embryo. *Development* **117**, 135-148.

Han, Y., Weinman, S., Boldogh, I., Walker, R. K. and Brasier, A. R. (1999). Tumor necrosis factor-alpha-inducible IkappaBalpha proteolysis mediated by cytosolic m-calpain. A mechanism parallel to the ubiquitin-proteasome pathway for nuclear factor-kappab activation. *J. Biol. Chem.* **274**, 787-794.

Hecht, P. M. and Anderson, K. V. (1993). Genetic characterization of tube and pelle, genes required for signaling between Toll and dorsal in the specification of the dorsal-ventral pattern of the Drosophila embryo. *Genetics* **135**, 405-417.

Huang, H.-R., Chen, Z. J., Kunes, S., Chang, G.-D. and Maniatis, T. (2010). Endocytic pathway is required for Drosophila Toll innate immune signaling. *Proc. Natl. Acad. Sci. USA* **107**, 8322-8327.

Ip, Y. T., Kraut, R., Levine, M. and Rushlow, C. A. (1991). The dorsal morphogen is a sequence-specific DNA-binding protein that interacts with a long-range repression element in Drosophila. *Cell* **64**, 439-446.

Isoda, K. and Nusslein-Volhard, C. (1994). Disulfide cross-linking in crude embryonic lysates reveals three complexes of the Drosophila morphogen dorsal and its inhibitor cactus. *Proc. Natl. Acad. Sci. USA* **91**, 5350-5354.

Kanodia, J. S., Rikhy, R., Kim, Y., Lund, V. K., DeLotto, R., Lippincott-Schwartz, J. and Shvartsman, S. Y. (2009). Dynamics of the Dorsal morphogen gradient. *Proc. Natl. Acad. Sci. USA* **106**, 21707-21712.

Kearns, J. D. and Hoffmann, A. (2009). Integrating computational and biochemical studies to explore mechanisms in NF-{kappa}B signaling. *J. Biol. Chem.* **284**, 5439-5443.

Konrath, F., Witt, J., Sauter, T. and Kulms, D. (2014). Identification of new IkappaBalpha complexes by an iterative experimental and mathematical modeling approach. *PLoS Comput. Biol.* **10**, e1003528.

Li, C., Chen, S., Yue, P., Deng, X., Lonial, S., Khuri, F. R. and Sun, S.-Y. (2010). Proteasome inhibitor PS-341 (bortezomib) induces calpain-dependent IkappaB (alpha) degradation. *J. Biol. Chem.* **285**, 16096-16104.

Liberman, L. M., Reeves, G. T. and Stathopoulos, A. (2009). Quantitative imaging of the Dorsal nuclear gradient reveals limitations to threshold-dependent patterning in Drosophila. *Proc. Natl. Acad. Sci. USA* **106**, 22317-22322.

Liu, Z.-P., Galindo, R. L. and Wasserman, S. A. (1997). A role for CKII phosphorylation of the cactus PEST domain in dorsoventral patterning of the Drosophila embryo. *Genes Dev.* **11**, 3413-3422.

Lund, V. K., DeLotto, Y. and DeLotto, R. (2010). Endocytosis is required for Toll signaling and shaping of the Dorsal/NF-kappaB morphogen gradient during Drosophila embryogenesis. *Proc. Natl. Acad. Sci. USA* **107**, 18028-18033.

Marek, L. R. and Kagan, J. C. (2012). Phosphoinositide binding by the Toll adaptor dMyD88 controls antibacterial responses in Drosophila. *Immunity* **36**, 612-622.

Mitchell, S., Vargas, J. and Hoffmann, A. (2016). Signaling via the NFkappaB system. *Wiley Interdiscip. Rev. Syst. Biol. Med.* **8**, 227-241.

Mizutani, C. M., Nie, Q., Wan, F. Y. M., Zhang, Y. T., Vilmos, P., Sousa-Neves, R., Bier, E., Marsh, J. L. and Lander, A. D. (2005). Formation of the BMP activity gradient in the Drosophila embryo. *Dev. Cell* **8**, 915-924.

O'Connell, M. D. and Reeves, G. T. (2015). The presence of nuclear cactus in the early Drosophila embryo may extend the dynamic range of the dorsal gradient. *PLoS Comput. Biol.* **11**, e1004159.

O'Dea, E. L., Barken, D., Peralta, R. Q., Tran, K. T., Werner, S. L., Kearns, J. D., Levchenko, A. and Hoffmann, A. (2007). A homeostatic model of IkappaB metabolism to control constitutive NF-kappaB activity. *Mol. Syst. Biol.* **3**, 111.

Packman, L. C., Kubota, K., Parker, J. and Gay, N. J. (1997). Casein kinase II phosphorylates Ser468 in the PEST domain of the Drosophila IkappaB homologue cactus. *FEBS Lett.* **400**, 45-50.

Pando, M. P. and Verma, I. M. (2000). Signal-dependent and -independent degradation of free and NF-kappa B-bound IkappaBalpha. *J. Biol. Chem.* **275**, 21278-21286.

Papatsenko, D. and Levine, M. (2005). Quantitative analysis of binding motifs mediating diverse spatial readouts of the Dorsal gradient in the Drosophila embryo. *Proc. Natl. Acad. Sci. USA* **102**, 4966-4971.

Development (2017) 144, 2907-2913 doi:10.1242/dev.145557

Reach, M., Galindo, R. L., Towb, P., Allen, J. L., Karin, M. and Wasserman, S. A. (1996). A gradient of cactus protein degradation establishes dorsoventral polarity in the Drosophila embryo. *Dev. Biol.* **180**, 353-364.

Reeves, G. T., Trisnadi, N., Truong, T. V., Nahmad, M., Katz, S. and Stathopoulos, A. (2012). Dorsal-ventral gene expression in the Drosophila embryo reflects the dynamics and precision of the dorsal nuclear gradient. *Dev. Cell* **22**, 544-557.

Roth, S. (2001). Drosophila oogenesis: coordinating germ line and soma. *Curr. Biol.* **11**, R779-R781.

Roth, S., Hiromi, Y., Godt, D. and Nusslein-Volhard, C. (1991). cactus, a maternal gene required for proper formation of the dorsoventral morphogen gradient in Drosophila embryos. *Development* **112**, 371-388.

Rushlow, C. A. and Shvartsman, S. Y. (2012). Temporal dynamics, spatial range, and transcriptional interpretation of the Dorsal morphogen gradient. *Curr. Opin. Genet. Dev.* **22**, 542-546.

Schaecher, K., Goust, J. M. and Banik, N. L. (2004). The effects of calpain inhibition on IkB alpha degradation after activation of PBMCs: identification of the calpain cleavage sites. *Neurochem. Res.* **29**, 1443-1451.

Shelton, C. A. and Wasserman, S. A. (1993). pelle encodes a protein kinase required to establish dorsoventral polarity in the Drosophila embryo. *Cell* **72**, 515-525.

Shen, J., Channavajhala, P., Seldin, D. C. and Sonenshein, G. E. (2001). Phosphorylation by the protein kinase CK2 promotes calpain-mediated degradation of IkappaBalpha. *J. Immunol.* **167**, 4919-4925.

Shimmi, O., Umulis, D., Othmer, H. and O'Connor, M. B. (2005). Facilitated transport of a Dpp/Scw heterodimer by Sog/Tsg leads to robust patterning of the Drosophila blastoderm embryo. *Cell* **120**, 873-886.

Shumway, S. D., Maki, M. and Miyamoto, S. (1999). The PEST domain of IkappaBalpha is necessary and sufficient for in vitro degradation by mu-calpain. *J. Biol. Chem.* **274**, 30874-30881.

Stathopoulos, A. and Levine, M. (2002). Dorsal gradient networks in the Drosophila embryo. *Dev. Biol.* **246**, 57-67.

Stein, D. S. and Stevens, L. M. (2014). Maternal control of the Drosophila dorsal-ventral body axis. *Wiley Interdiscip. Rev. Dev. Biol.* **3**, 301-330.

Sun, H., Towb, P., Chiem, D. N., Foster, B. A. and Wasserman, S. A. (2004). Regulated assembly of the Toll signaling complex drives Drosophila dorsoventral patterning. *EMBO J.* **23**, 100-110.

Umulis, D. M., Serpe, M., O'Connor, M. B. and Othmer, H. G. (2006). Robust, bistable patterning of the dorsal surface of the Drosophila embryo. *Proc. Natl. Acad. Sci. USA* **103**, 11613-11618.

Whalen, A. M. and Steward, R. (1993). Dissociation of the Dorsal-Cactus complex and phosphorylation of the dorsal protein correlate with the nuclear localization of Dorsal. *J. Cell Biol.* **123**, 523-534.

Cardoso et al. Supplementary data

Supplementary Table I

***cactus* maternal genotypes studied and their effect on cuticle and on embryo viability**.

maternal genotype	embryo viability	cuticle phenotype	severity
cact[011]/+	100% viable	NA	0
cact[A2]/+	70%	WT (Fontenele 2013)	0
Df(2L)*cact*255/+	-	WT or V4	0
cact[011]/ *cact*[011]	-	V3 (Roth 1991)	+
cact[A2]/ *cact*[A2]*	-	V2 (Roth 1991)	+++
cact[A2]/ *cact*[011]	0% (n>500)	V3 or V2	++
cact[A2]/ *cact*[4]**	0% (n>500)	V2	+++
cact[011]/ Df(2L)*cact*255	0% (n>500)	V3 or V2	++
cact[A2]/ Df(2L)*cact*255	0% (n=525)	V2 or V1	+++
cact[A2]/ Df(2L)III18	0% (n>500)	-	+++
cact[A2]/ *dl*[6]	55% (n=800)	WT or V4	NA
cact[4]/ *dl*[6]	79% (n=138)	-	NA
dl[6]/+	97%	WT (Araujo and Bier, 2000)	NA
cact[E10]/ *cact*[A2]	0% (n>500)	L2-D1 (Roth 1991)	NA

Cuticle phenotypes are as in Roth et al, 1991, where ventralization increases V4<V3<V2<V1, and corresponds to expansion of ventro-lateral cuticle rich in denticles and progressive loss of dorso-lateral and dorsal structures.

Severity is defined as the degree of phenotypic strength due to loss of Cact activity, based on the ensemble of effects on cuticle, protein levels and viability.

* With current *cact*[A2] strains obtained either from the stock center or directly from researchers we were unable to generate homozygous *cact*[A2] adults.

**_cact_[A2]/_cact_[4] is semilethal, but _cact_[4]/Df(2L)III18 is lethal, thus this maternal genotype is not presented in the table.

NA not applicable

Supplementary Figure 1

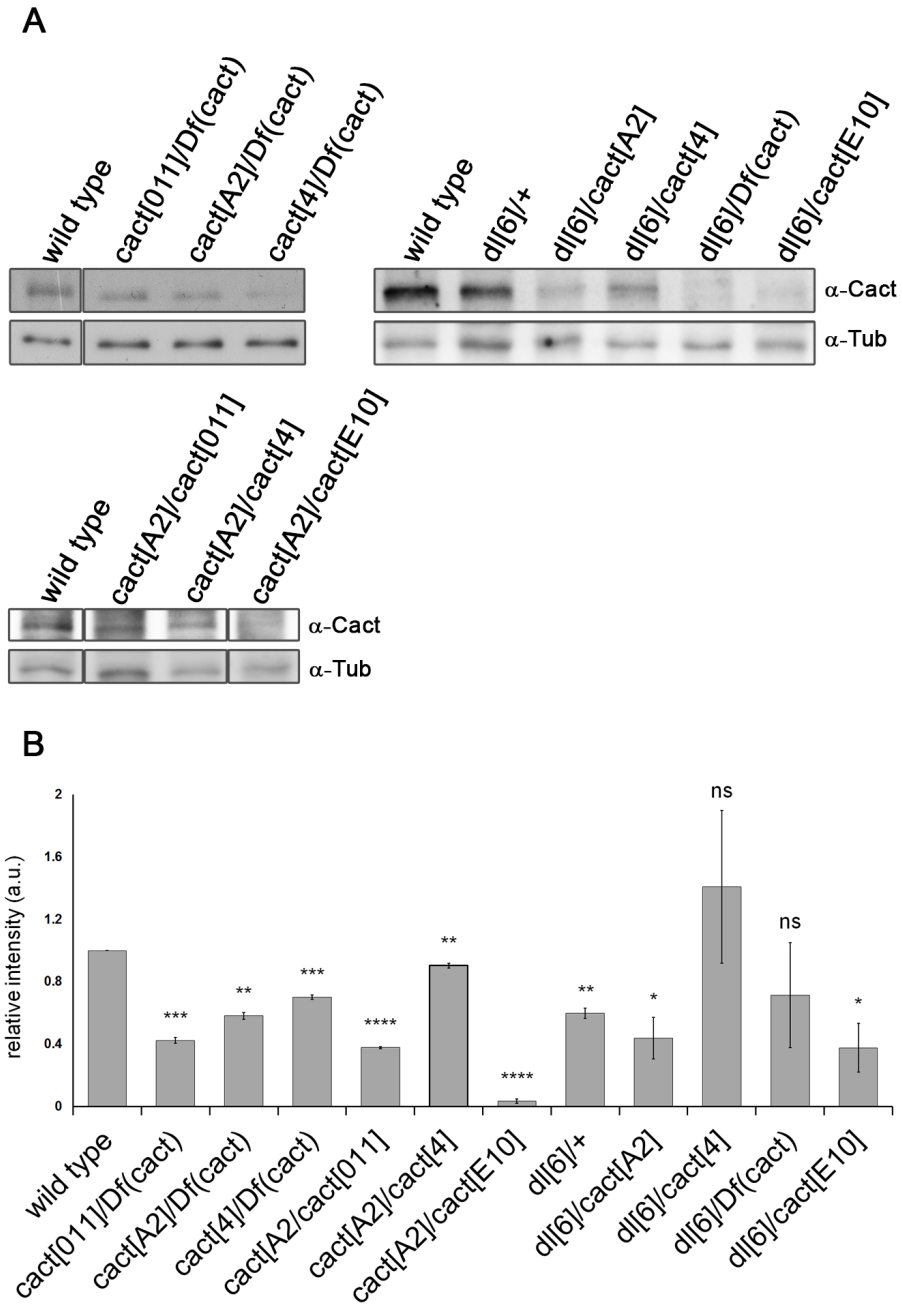

Cactus protein levels in 30min-1h30min old embryos, resulting from maternal loss-of-function allelic combinations. Three representative western blots (A) and quantification (B) of fullb length Cact protein levels in the different heteroallelic combinations with *dorsal* and *cact* alleles as well as deficiencies used

in this study. Three different samples were prepared and analyzed for each genotype. Normalized Cactus levels were calculated using the Tubulin loading control. Cact levels in single heterozygotes for the different alleles are not shown since they result in no significant alteration in Cact protein levels. Lower Mw Cact[E10] is not shown in the blots, but is present in amounts comparable to wild type Cact levels in *cact*[A2]/*cact*[E10] and *dl*[6]/*cact*[E10]. Statistically significant differences based on Student's t-test and displayed as mean±s.e.m. (****P≤0.0001***P≤0.001, **P≤0.01, *P≤0.05).

Supplementary Figure 2

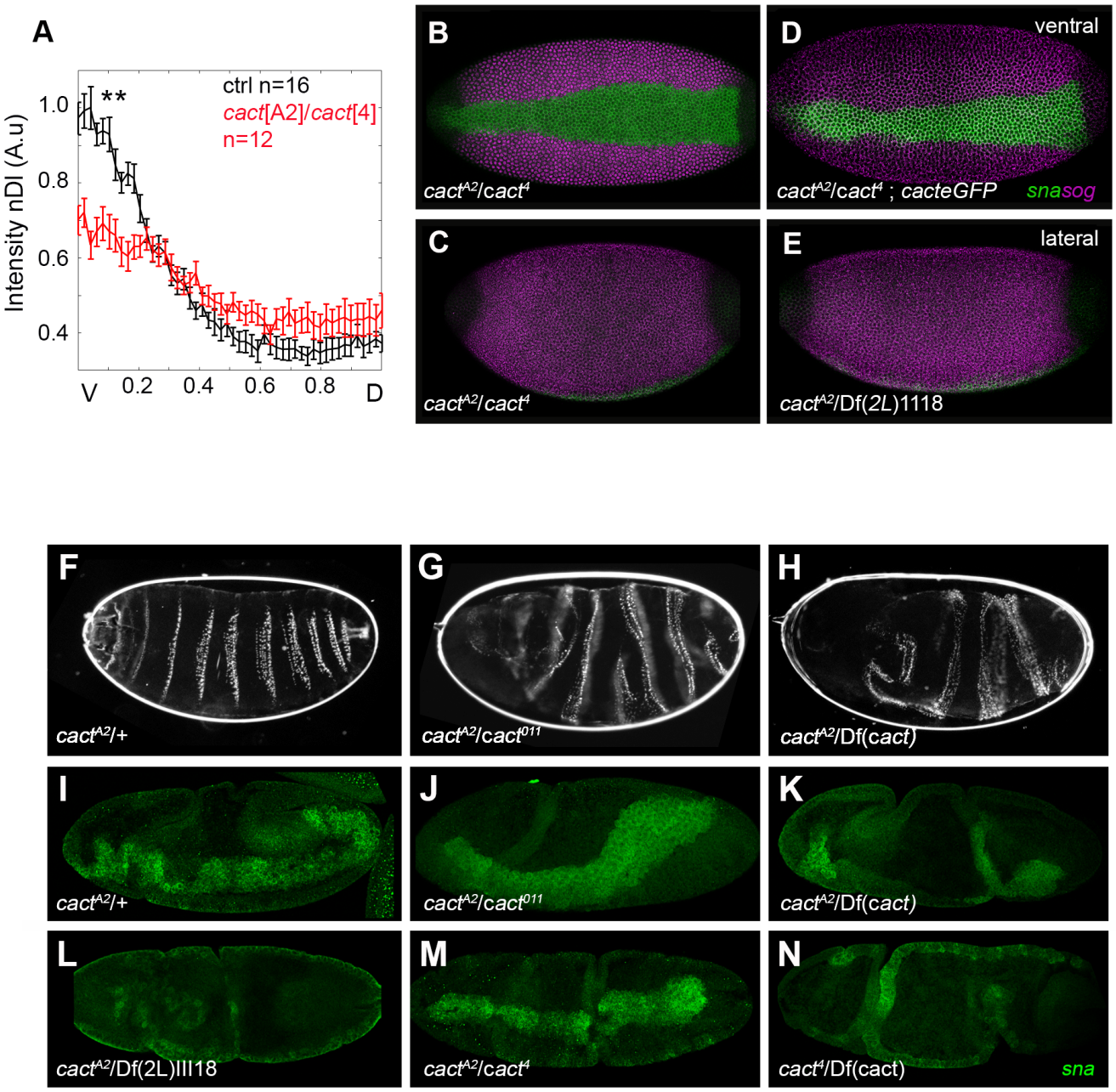

Loss of *cact* activity reduces nDl in ventral regions of the embryo. In (A) embryos from *cact*[A2]/*cact*[4] (red) mothers. The amount of nuclear Dl decreases in ventral regions of the embryo and increases in lateral regions,

respective to control embryos (black). B-E) *in situ* hybridization for *sna* and *sog* in *cact*[A2]/*cact*[4] (B,C), *cact*[A2]/*cact*[4]; *cact-eGFP*/+ (D) and *cact*[A2]/Df(2L)III18 (E) embryos shows that loss of *cact* reduces ventral *sna* and widens lateral *sog*. *cacteGFP* overexpression produces no effect on *cact*[A2]/*cact*[4] *sog* and *sna* domains. Fb H) Cuticle pattern for *cact*[A2]/+ showing a wild type phenotype, (F), *cact*[A2]/*cact*[011] with a characteristic V2 ventralized pattern (G), and *cact*[A2]/Df(cact) ventralized cuticles that are slightly elongated (H). Ib N) *in situ* hybridization for *sna* or *twi* (K), in gastrulation stage embryos. The internal mesoderm layer is clearly seen in *cact*[A2]/+ (I) and *cact*[A2]/*cact*[011] (J), reduced in *cact*[A2]/Df(cact) (K), and sometimes almost absent in *cact*[A2]/Df(2L)III18 (L), *cact*[A2]/*cact*[4] (M) and *cact*[4]/Df(cact) (N). The gastrulation pattern is also abnormal in Jb N. Ventral views in B,D,F,L,M, lateral views in C,E,I,J,K,N. Anterior is left and posterior is right in all panels.

Supplementary Figure 3

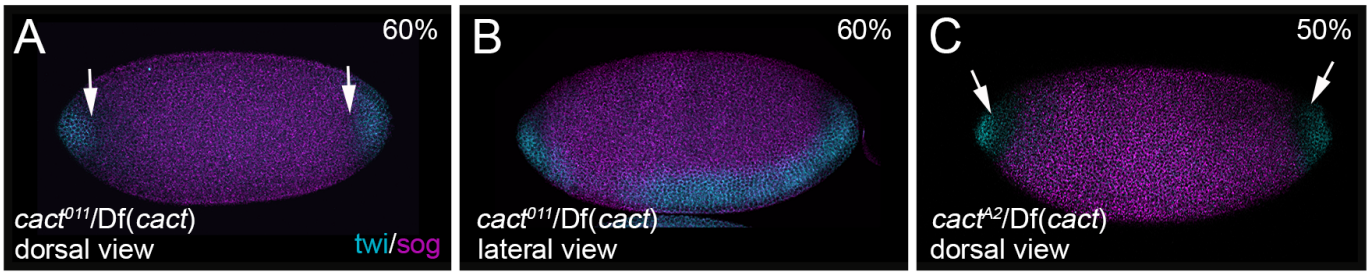

***cact* loss of-function mutants alter the ventral domain of *twist* expression**. It has been reported that in embryos from homozygous mothers carrying a viable loss-of-function *cact* allele, the ventral *twist* domain expands dorsally at the anterior and posterior tips of the embryo (Roth et al, 1991). Accordingly, we observe a small anterior-posterior expansion of *twist* in *cact*[011]/Df(*cact*) (A) in addition to a loss of ventral *twist* expression (B). Contrarily, in embryos from *cact*[A2]/Df(*cact*) mothers, no anterior-posterior expansion is observed (C). A,C are dorsal views, B is a ventral-lateral view. Anterior is left, posterior to the right.

Supplementary Figure 4

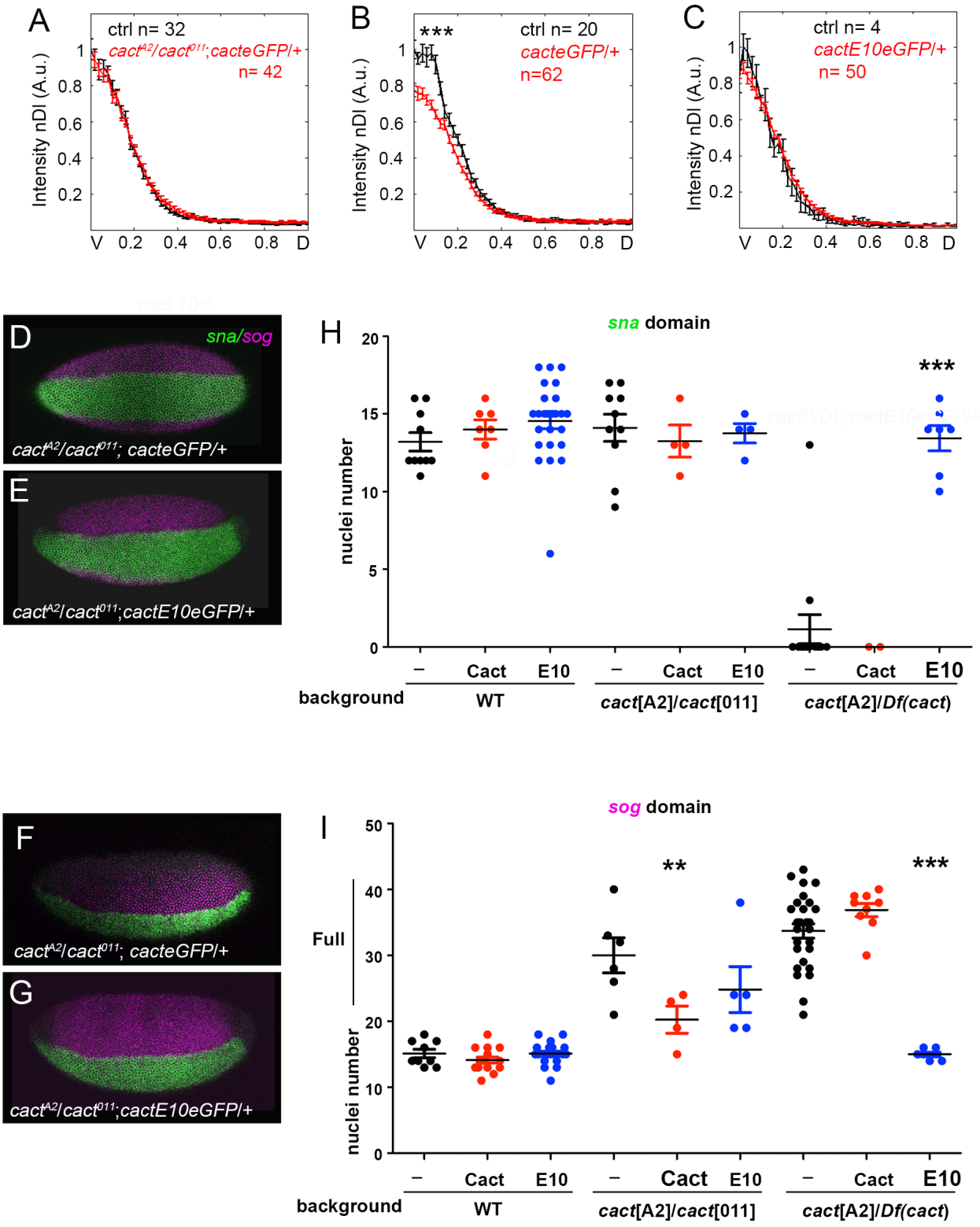

Full-length Cact and truncated Cact[E10] overexpression produce qualitatively different effects on the DV axis. A-C) Nuclear Dl gradients for control embryos (black) or embryos from *cact[A2]/cact[011]; cact-eGFP/+* (A), *cact-eGFP/+* (B) or *cactE10-eGFP/+* (C) mothers (red). When endogenous Cact is reduced (A), Cact-eGFP recovers nDl to a wild type pattern (compare to Fig 1C). Overexpression of full-length Cact-eGFP slightly decreases nDl in a wild type background (B), while Cact[E10]-eGFP has no effect (C). D-G) *in situ* hybridization for *sna* and *sog* in *cact*[A2]/*cact*[011]; *cact-eGFP*/+ (D,F); *cact*[A2]/*cact*[011]; *cactE10-eGFP*/+ (E,G) embryos and (H,I) quantification of *sna* (H) and *sog* (I) in these different genotypes, plus *cact*[A2]/Df(*cact)*; *cact-eGFP*/+ and *cact*[A2]/Df(*cact*); *cactE10-eGFP*/+ from Fig 3 for direct comparison. The size of the *sog* domain is defined as "full" expansion when it expands completely to the dorsal side and no dorsal *zen* expression is observed. Differences are statistically significant based on Student's t-test and displayed as mean±s.e.m. (***P<0.001, **P<0.01). Interestingly, Cact-eGFP is able to generate CactE10-eGFP but does not enhance nDl levels ventrally in *cact*[A2]/Df(*cact*), unlike CactE10-eGFP. This is possibly a matter of stoichiometry between Cact-eGFP and CactE10-eGFP. By inducing *cact-eGFP* expression we increase both full length Cact-eGFP and CactE10-eGFP, generated by the action of CalpA. By expressing *cactE10-eGFP* we skew this proportion towards a greater ratio of E10/WT forms.

Supplementary Figure 5

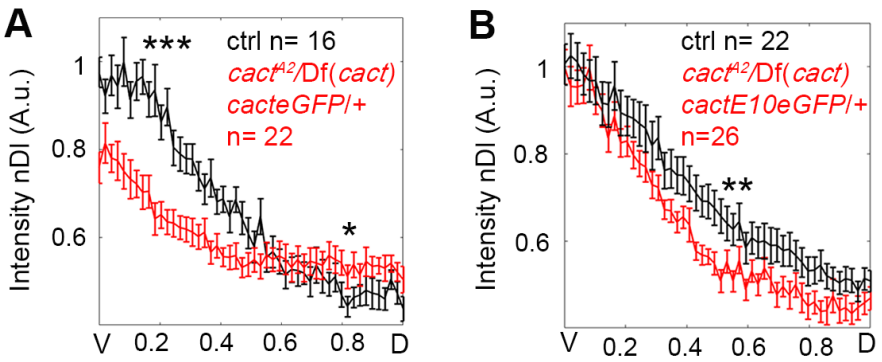

Cact[E10] exerts positive and inhibitory effects on the nDl gradient when endogenous wild type *cact* is reduced. nDl gradients resulting from overexpression of Cact-eGFP (A) or Cact[E10]-eGFP (B) in a *cact*[A2]/Df(*cact*) background (compare to Fig 1D) shows that Cact-eGFP does not alter the *cact*[A2]/Df(*cact*) nDl gradient in ventral regions, while Cact[E10] almost recovers the wild type nDl pattern, consistent with *sna* and *sog* expression domains shown in Fig 3. Control gradients in black in both graphs.

Supplementary Figure 6

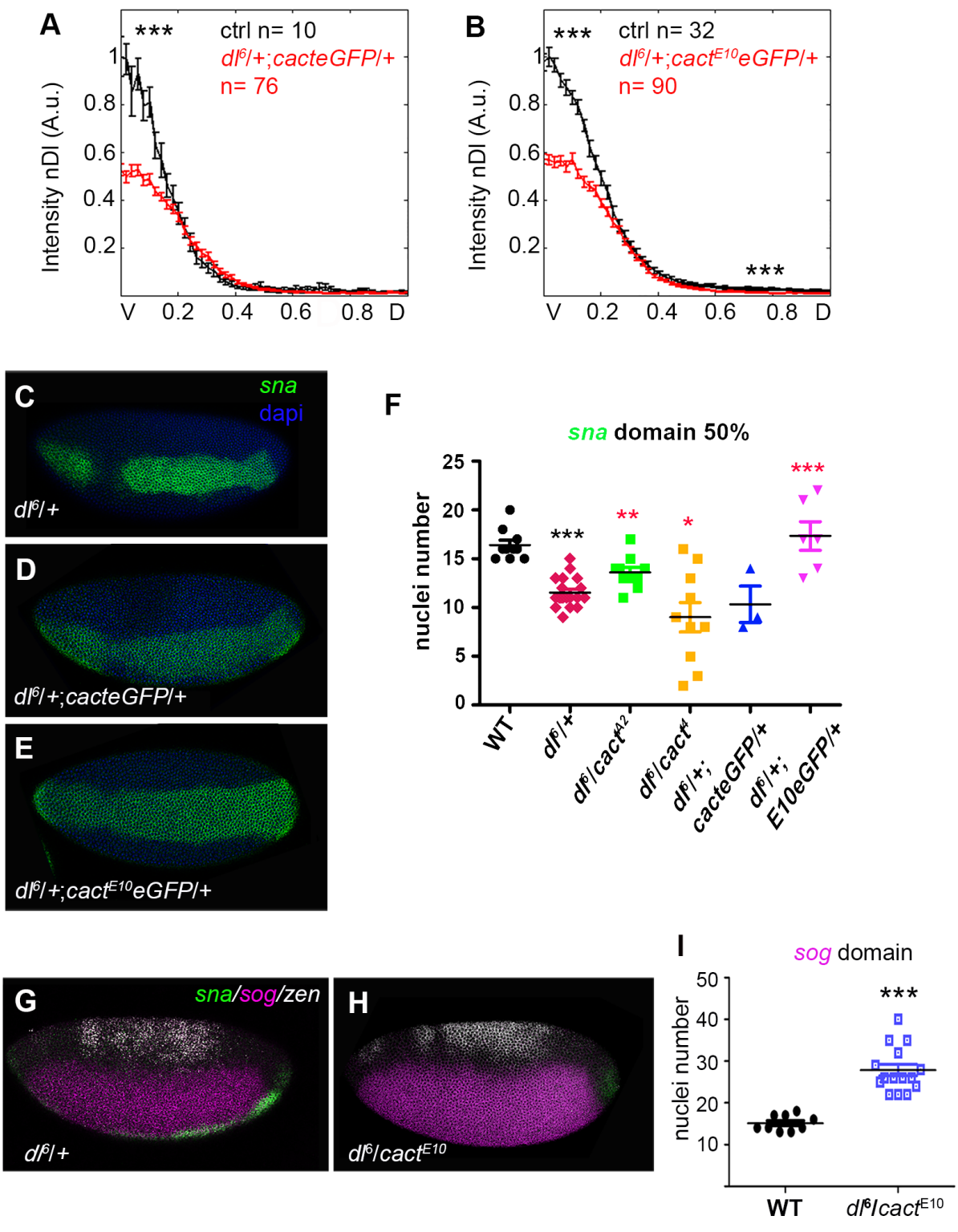

Cact[E10] exerts a strong effect on the nDl gradient when the amount of Dl is reduced. A,B) nDl gradients resulting from overexpression of Cact-eGFP (A) or Cact[E10]-eGFP (B) in a *dl*- heterozygous background. Control gradients in black in both graphs. Cb E) *in situ* hybridization for the ventral gene *sna* reveals that Cact[E10]b eGFP recovers the loss of the ventral *sna* domain observed in *dl*[6]/+ (E). This positive effect is also seen by quantification of the *sna* domain (F). Note that the *sna* domain in *dl*[6]/*cact*[A2] is stochastic, coinciding with *sog* expression as shown in Fig 2. Gb I) *in situ* hybridization for ventral *sna,* lateral *sog* and dorsal *zen* shows that the *cact*[E10] allele expands *sog* both ventrally and dorsally (H) in relation to *dl[*6]/+ (G), as quantified in (I), where the *sog* domain in *dl[*6]/+ is equivalent to wild type. Therefore, *cact*[E10] exerts a dual effect to enhance and to inhibit Toll responses. Differences are statistically significant based on Student's tb test and displayed as mean±s.e.m. (***P<0.001, **P<0.01).